JOURNAL OF CHEMICAL INFORMATION AND MODELING

ARTICLE

pubs.acs.org/jcim

Theoretical Modeling of Molecular Spectra Parameters of Disubstituted Diacetylenes

Maciej Roman,[†] Jan Cz. Dobrowolski,[‡,§] and Malgorzata Baranska*[,†]

[†]Faculty of Chemistry, Jagiellonian University, 3 Ingardena Street, 30-060 Kraków, Poland

[‡]Industrial Chemistry Research Institute, 8 Rydygiera Street, 01-793 Warsaw, Poland

[§]National Medicines Institute, 30/34 Chełmska Street, 00-725 Warsaw, Poland

Supporting Information

ABSTRACT: Symmetrically disubstituted diacetylenes, X-C≡C−C≡C-X, were studied computationally by using the DFT B3LYP/aug-cc-pVDZ method. For more than 35 substituents the bond lengths, charge density and Laplacian in bond critical points, C≡C stretching vibrational frequencies, ^{13}C NMR chemical shifts and spin−spin CC coupling constants through diacetylene moiety were calculated and examined by using the substituent sEDA and pEDA descriptors. It is demonstrated that in disubstituted diacetylenes the triple bond length increases with the electron donating and decreases with the electron withdrawing properties of the substituents. The σ-electron repulsion is likely to be responsible for this phenomenon. The electron density of the C-X bond critical point decreases linearly with an increase of the σ-electron donating properties, whereas the Laplacian of electron density in the C≡C bond critical point increases as the sEDA descriptor i.e., σ-electron donating properties of the substituent, are increased. Thus, ρ(C≡C) is locally reduced with an increase of sEDA. The ν_{as}(C≡C) and ν_{s}(C≡C) mode frequencies decrease with the electron donating and increase with the electron withdrawing properties of the substituents. The calculated chemical shift of the C1-atom, to which the substituent is attached, does not correlate with the substituent descriptors, whereas the δ(C2) deshielding increases when the σ-electron donating properties and C≡C distance are increased. The calculated ^{1}J(CC) coupling constants decrease with an increase of the triple bond length, the sEDA parameter, and ρ(C-X), whereas they decrease with Laplacian in the C≡C BCP.

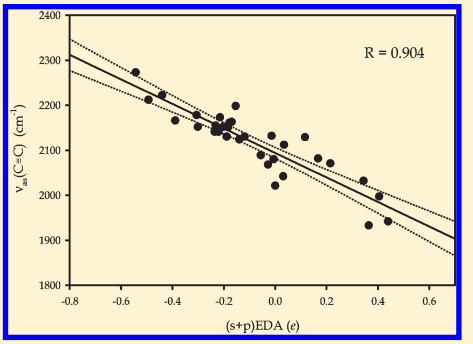

1. INTRODUCTION

Diacetylenes are successfully synthesized since the late 1860s.[1] Nowadays, very sophistically substituted diacetylenes can be prepared including metals and organometallic substituents.[2,3] They are valuable for obtaining conductive polydiacetylenes constituted by alternating triple and double bonds in *trans* configuration.[4−6] There is a huge natural occurrence of plant diacetylenes, classified as polyacetylenes, and now, the number of them reaches the thousands.[7−9] For instance, they occur in roots of carrot, parsley, celery, aster, daisy, or sunflower as well as in plants from East Asia like ginseng.[10−14] Simple diacetylenes have been discovered in interstellar space.[15−19]

Diacetylenes are difficult for experimental studies. Diiododiacetylene, synthesized by Baeyer in 1885,[20] explodes after heating over its melting point at 95 °C. The other dihalodiacetylenes are even less stable.[21] Isolation of natural diacetylenes is also difficult because extracted from tissues either oxidize or decompose under light or pH change.[7−9] Hence, physicochemical data of diacetylenes are very limited. For symmetrically disubstituted diacetylenes studies of substituent effect on IR and Raman or on ^{13}C NMR spectra were performed only for a small number of derivatives. A very strong and polarized Raman band of diacetylenes can be observed due to -C≡C−C≡C- symmetric stretching vibration at ca. 2200 cm^{-1}.[6,12,13,22−25] Because only rare functional groups scatter in this very region the presence of polyacetylenes in plant tissues can be done by *in situ* Raman mapping.[10−14] Both, the number of conjugated -C≡C- bonds in polyacetylenes and substituents influence the number of Raman bands, their frequencies, and intensities.[23,24] Thus, the shape of Raman spectrum in the region of ca. 2200 cm^{-1} allows recognition of the type of substituent and identification of polyacetylene type. On the other hand, the ^{13}C NMR spectra analysis is of fundamental importance for both: natural polyacetylenes analysis and synthesized diacetylene characterization.

The aim of this study is to examine substituent influence on diacetylene moiety structure and electron density as well as its characteristics in IR, Raman, and ^{13}C NMR spectra. Taft and Topsom distinguish four components of substituent effect:[26,27] (i) the field-inductive component (F), (ii) electronegativity (EN), (iii) polarizability (P), and (iv) resonance (R). The substituent constants were correlated with atomic charges,[28−30] electrostatic potential,[31] NMR shifts,[32] and the π electron delocalization.[33] Recently, we constructed two computational substituent effect descriptors, sEDA

Received: September 9, 2010
Published: January 21, 2011

dx.doi.org/10.1021/ci1003587 | *J. Chem. Inf. Model.* 2011, 51, 283–295

Table 1. C≡C and C−C Bond Lengths d(C≡C) and d(C−C) (Å) and α and β Angles (α=180°-a(R-C1≡C2) and β=180°-a-(C1≡C2−C3)) Expressing Deviation from Linearity of the Symmetrically Disubstituted Diacetylene System Calculated at the B3LYP/aug-cc-pVDZ Level[a]

R = substituent	d(C≡C) (Å)	d(C−C) (Å)	α (deg)	β (deg)	sEDA (e)	pEDA (e)	(s+p)EDA (e)
Li	1.247	1.372	0.00	0.00	0.460	−0.020	0.440
MgH	1.239	1.368	0.00	0.00	0.424	−0.019	0.405
Na	1.247	1.376	0.00	0.00	0.377	−0.013	0.364
BeH	1.236	1.364	0.00	0.00	0.396	−0.052	0.344
$SiMe_3$	1.230	1.369	0.00	0.00	0.230	−0.015	0.215
SiH_3	1.228	1.367	0.00	0.00	0.184	−0.017	0.167
BF_2	1.225	1.362	0.00	0.00	0.193	−0.077	0.116
$MeSO_2$	1.221	1.364	5.95	2.57	0.016	0.018	0.034
BH_2	1.240	1.346	0.00	0.00	0.173	−0.142	0.031
H	1.217	1.371	0.00	0.00	0.000	0.000	0.000
H exp.	1.210	1.373	0.00	0.00	0.000	0.000	0.000
MeSO	1.225	1.362	11.21	3.12	−0.024	0.018	−0.006
SO_2F	1.219	1.362	5.49	2.22	0.012	−0.026	−0.014
MeS	1.231	1.355	4.56	3.25	−0.134	0.106	−0.028
SH	1.228	1.358	7.76	2.97	−0.149	0.093	−0.056
$COCH_3$	1.224	1.361	1.56	3.11	−0.119	0.000	−0.119
Br	1.221	1.365	0.00	0.00	−0.197	0.057	−0.140
CF_3	1.215	1.366	0.00	0.00	−0.130	−0.024	−0.154
CFO	1.221	1.359	4.52	3.06	−0.088	−0.081	−0.169
COOH	1.220	1.361	5.78	3.07	−0.110	−0.068	−0.178
$CONH_2$	1.221	1.364	5.66	2.76	−0.140	−0.044	−0.184
CHO	1.224	1.359	4.31	3.69	−0.102	−0.087	−0.189
CN	1.225	1.354	0.00	0.00	−0.159	−0.035	−0.196
Cl	1.219	1.365	0.00	0.00	−0.264	0.062	−0.202
CH_3	1.220	1.371	0.00	0.00	−0.229	0.014	−0.215
$CHCH_2$ (C_{2v})	1.226	1.361	3.61	3.59	−0.213	−0.008	−0.221
$CHCH_2$ (C_{2h})	1.226	1.361	3.72	2.75	−0.213	−0.008	−0.221
Ph	1.225	1.362	0.00	0.00	−0.232	0.001	−0.231
tBu	1.221	1.371	0.00	0.00	−0.240	0.008	−0.232
COCN	1.223	1.357	2.07	2.74	−0.119	−0.117	−0.236
NMe_2	1.230	1.358	2.03	0.20	−0.475	0.174	−0.301
NH_2	1.226	1.361	3.94	2.81	−0.451	0.145	−0.306
NO_2	1.217	1.358	0.00	0.00	−0.320	−0.069	−0.389
NO	1.347	1.231	0.00	0.00	−0.264	−0.129	−0.393
OH	1.217	1.369	8.44	0.24	−0.561	0.121	−0.440
COOMe	1.217	1.367	6.27	2.64	−0.546	0.052	−0.494
OCF_3	1.214	1.367	7.90	3.99	−0.533	0.035	−0.497
OCN	1.213	1.366	0.00	0.00	−0.595	0.070	−0.525
F	1.210	1.373	0.00	0.00	−0.621	0.078	−0.543

[a] sEDA, pEDA, and (s+p)EDA are substituent effect descriptors.[34,35].

and pEDA, measuring an extent the σ- and π-electrons are donated or withdrawn by a substituent.[34,35] The sEDA descriptor correlates fairly well with the Boyd and Boyd/Boyd-Edgecombe[36,37] and Marriott et al.[38] EN scales, while the pEDA descriptor correlates definitely well with the Taft and Topsom[26] and fairly well with Swain and Lupton[39] resonance effect scales. The descriptors appeared to be useful for substituted methanes, ethenes, diazoles, and triazoles. According to Taft and Topsom terms[26,27] the sEDA and pEDA descriptors measure two out of four substituent effect components: electronegativity and resonance, respectively.

The paper is structured as follows: Section 3.1 refers to structure of symmetrically disubstituted diacetylene moiety, Section 3.2 discusses electron density properties in bond critical points, Section 3.3 deals with the theoretical prediction of vibrational frequencies and IR and Raman intensities, and Section 3.4 reports on ^{13}C NMR chemical shifts and coupling constants.

2. THEORETICAL CALCULATIONS

All calculations were done with the B3LYP DFT functional[40] combined with the Dunning type cc-pVDZ and aug-cc-pVDZ basis sets[41,42] using the Gaussian 09 program.[43] The Dunning basis sets are known to adequately describe the organic molecules and

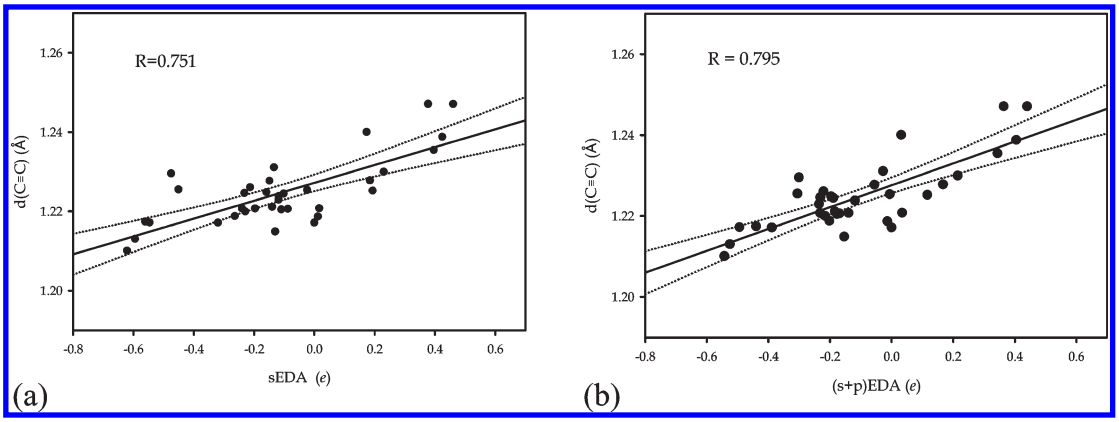

Figure 1. Linear regression between the B3LYP/aug-cc-pVDZ calculated triple bond length d(C≡C) of symmetrically disubstituted diacetylenes and (a) sEDA and (b) (s+p)EDA descriptors (R = 0.751 and 0.795, respectively). Dotted lines show the regression bands at the 95% confidence level.

their interactions.[44] Inspection of a number of imaginary frequencies checked for each structure guaranteed that only true minima on PES were analyzed. Total energies and Gibbs free energies are listed in Table 1SI. If more than one conformer was found, then data for the most stable one were taken for further analysis. For the studied structures the conformation variation has negligible impact on data and correlations. Thus, for presentation clarity the conformational changes are not discussed. The Atoms-in-Molecules (AIM) analysis[45] (Table 2SI) was performed by using the AIM2000 program.[46]

The ^{13}C chemical shifts of i-th nuclei δ(i)[47,48] and spin−spin coupling constants (SSCC) ^{k}J(CC), k = 1−4,[49] were calculated at the B3LYP level by using the DFT-GIAO routine,[50] setting the aug-cc-pVDZ-su1 basis set for the C atoms and the aug-cc-pVDZ basis for the other elements. The chemical shifts were calculated as δ(i) = σ(TMS) - σ(i) where σ(i) and σ(TMS) are isotropic parts of shielding tensors of i-th nuclei and TMS, respectively. The aug-cc-pVDZ-su1 basis set was constructed from the aug-cc-pVDZ basis sets by deconstructing the s functions and adding tight s orbital, as suggested in ref 51. Former studies[52,53] indicated this type of basis sets to better reproduce the SSCCs.

3. RESULTS AND DISCUSSION

3.1. Geometry. The C≡C and C−C bond lengths in diacetylenes change with a change of substituent (Table 1). Indeed, the C≡C bond length tends to increase with an increase of the σ electron donating properties of the substituent expressed by the sEDA descriptor (R = 0.751, Figure 1a), while an analogous correlation with pEDA descriptor (expressing π-electron donating properties) is statistically insignificant. Remarkably, the correlation with the (s+p)EDA descriptor (summarizing the σ and π electrons effects) is slightly improved (R = 0.795, Figure 1b). The substituent influence on diacetylene C−C single bond length is insignificant (Table 1). Branched substituents may cause nonlinearity of the R-C≡C and C≡C−C angles; however, no regular dependence between the angles and descriptors is observed.

Surprisingly, the triple bond length increases with the electron donating and decreases with the electron withdrawing properties of the substituents. Indeed, the higher the carbon−carbon bond order, the shorter the bond, i.e. d(C−C) ≈ 1.55 Å, d(C═C) ≈ 1.35 Å, and d(C≡C) ≈ 1.20 Å. However, the π electrons are responsible for the bond order, while changes of the charge density in the -C≡C−C≡C- systems are mostly due to substituent interaction through the σ electrons (Figure 1a). Moreover, the tendency occurs within bond length changes of only 0.05 Å. The σ-electron repulsion in the space of C≡C bonds is likely to be responsible for this phenomenon. The repulsion decreases, when electrons are taken out from the space of the C≡C bonds and the bond is strengthened and shortened, whereas it increases, when the electrons are donated to the system and the valence electron repulsion increases and so do the C≡C bonds.

3.2. Electron Density. The electron density (ρ), Laplacian of the electron density ($\nabla^2\rho$), and elipticity (ε) in bond critical points of the diacetylene moiety (BCPs in C≡C, C−C, and C-X, Table 2SI) were examined by the AIM method for whether they follow the variation of the valence σ and π electron population of the diacetylene moiety changed by the substituent or not.

The electron density in the C≡C and C−C BCPs changes but within only 0.02 au. Out of several possible correlations parameters in diacetylene BCPs and sEDA and pEDA descriptors, the linear decrease of ρ(C-X) with an increase of sEDA is found to be significant; however, the correlation with (s+p)EDA is a bit stronger (R = 0.908, Figure 2a). Thus, ρ(C-X) tends to decrease with increasing overall electron donating properties of the substituent. This is logical since the electron density is pushed by a substituent more and more off the X-C bond to the diacetylene system.

For Laplacians, only $\nabla^2\rho$(C≡C) increases with an increase of (s+p)EDA (R = 0.907, Figure 2b). The Laplacian of ρ is positive when ρ is locally reduced, while negative if it is locally concentrated.[45] Thus, ρ(C≡C) is definitely locally depleting with an increase of overall electron donating properties of the substituent. A weak, linear correlation between $\nabla^2\rho$(C−C) and d(C−C) (R = 0.693) shows, that, in harmony with chemical intuition, the ρ(C−C) is reduced as the single bond length is increased.

The elipticity in the C≡C, C−C, and C-X bonds was expected to reflect the bond order changes with a substituent; however, no statistically significant correlations with sEDA and pEDA descriptors were found.

3.3. Vibrational Spectra of Diacetylenes. *3.3.1. Diacetylene.* Two C≡C oscillators in diacetylene H−C≡C−C≡C−H are coupled and their characteristic symmetric ν_s(C≡C) and asymmetric ν_{as}(C≡C) modes manifest themselves at 2188.9 and

dx.doi.org/10.1021/ci1003587 |J. Chem. Inf. Model. 2011, 51, 283–295

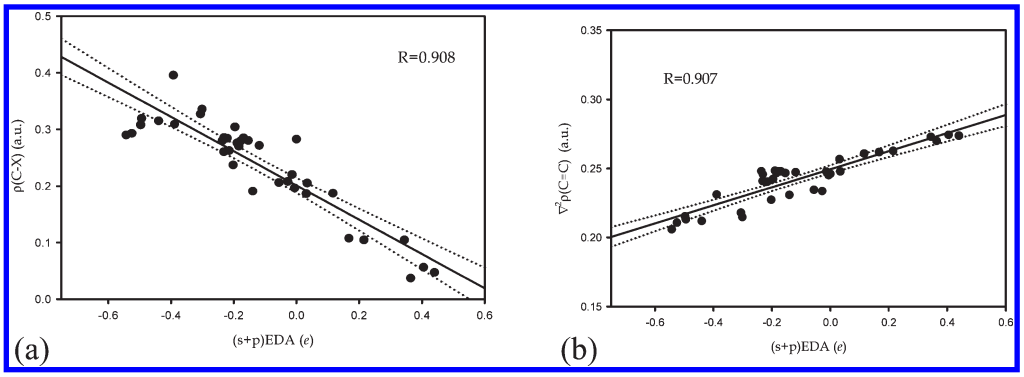

Figure 2. Linear regression of the electron density in the C-X BCP (a) and Laplacian at C≡C BCP (b) in symmetrically disubstituted diacetylenes and (s+p)EDA descriptor. Dotted lines show the regression bands at the 95% confidence level.

Table 2. Experimental and Theoretical ν_{as}(C≡C) and ν_s(C≡C) IR and Raman Frequencies (ν, cm^{-1}) and IR and Raman Intensities (I_{IR}, km mol^{-1} and A_R, A^4 amu^{-1}, Respectively) of the Diacetylene Molecule

	asymmetric stretching ν_{as}(C≡C)			symmetric stretching ν_s(C≡C)			
method	ν	I_{IR}	A_R	ν	I_{IR}	A_R	no. of basis functions
Exp. anh.[54]	2022.2			2188.9			
Exp. harm.[56]	2050			2222			
AE-CCSD(T)/ cc-pCVQZ[56]	2064.0			2243.0			
B3LYP							
cc-pVDZ	2115.2	1.1994	0.000	2289.5	0.000	669.522	66
cc-pVTZ	2113.3	2.8297	0.000	2281.4	0.000	789.092	148
cc-pVQZ	2109.7	4.2163	0.000	2276.3	0.000	876.143	280
cc-pV5Z	2108.7	5.3845	0.000	2275.5	0.000	952.067	474
aug-cc-pVDZ	2105.6	5.4340	0.000	2281.0	0.000	1014.771	110
aug-cc-pVTZ	2111.2	5.5061	0.000	2278.4	0.000	999.820	230
aug-cc-pVQZ	2108.7	5.6268	0.000	2275.6	0.000	999.702	412

2022.2 cm^{-1}, respectively.[54−58] Diacetylene molecule belongs to the D_{4h} point symmetry group and exhibits the symmetry center, thus, ν_s(C≡C) mode is active in Raman and inactive in IR spectrum and ν_{as}(C≡C) oppositely (Table 2). The basis set size has only small influence on frequencies of the two modes. Indeed, an extension of the basis set from cc-pVDZ to cc-pV5Z (148 and 474 basis functions, respectively) results in the ν_s(C≡C) and ν_{as}(C≡C) modes shift not greater than 15 cm^{-1} (Table 2). Hence, the experimental harmonic frequencies can be fairly reproduced using the cc-pVDZ basis set. However, the theoretical ν_s(C≡C) and ν_{as}(C≡C) Raman and IR band intensities depend strongly on the basis set size:[59,60] the Raman activity of the ν_s(C≡C) mode is 669.5 A^4/amu for the cc-pVDZ basis set, whereas it is 952.1 A^4/amu for the cc-pV5Z one (Table 2). The IR intensity of the ν_{as}(C≡C) mode changes even more: from 1.2 km/mol to 5.4 km/mol, respectively. Addition of the diffuse functions yields, however, a positive result. The aug-cc-pVDZ basis set of fairly reasonable size yields intensities quite similar to those obtained with 4-times larger aug-cc-pVQZ basis set. Therefore, henceforth, we refer mostly to the B3LYP/aug-cc-pVDZ results.

3.3.2. Symmetrically Substituted Diacetylenes. Diacetylene derivative, if symmetrically disubstituted with a small substituent (e.g, Cl, Me, Ph), often preserves the symmetry center and still one of the two ν_s(C≡C) and ν_{as}(C≡C) modes is observed in Raman and the other in IR spectrum. However, if diacetylene is substituted by a substituent of mass similar to that of the -C≡C- moiety, several additional couplings occur and the spectral picture in the ν(C≡C) region is complicated. For instance, for CN, C≡C−H, or NO disubstitutions the two ν_s(C≡C) and ν_{as}(C≡C) modes cannot be recognized and different bands appear in the region. Further, when the symmetry center is released as an effect of specific substituent conformations, the two -C≡C- stretching modes become active in each of the vibrational spectra. Although, many factors influence the disubstituted diacetylene ν(C≡C) bands, we show that using the sEDA and pEDA descriptors the band frequencies do correlate with the substituent properties.

3.3.3. The ν(C≡C) Mode Frequencies. Upon symmetrical disubstitution, at the B3LYP/aug-cc-pVDZ level, the diacetylene ν_{as}(C≡C) and ν_s(C≡C) band frequencies change by over 300 cm^{-1}, the former from 1933 cm^{-1} (Na) to 2273 cm^{-1} (F) and the later from 2064 cm^{-1} (BH_2) to 2373 cm^{-1} (F) (Table 3, scaling factor of 0.960). Juxtaposition of the experimental[55−58,61−69] and scaled theoretical ν(C≡C) frequencies of selected diacetylenes is given in Table 4. In the C≡N, N═O, and OCN disubstituted diacetylenes, the substituent stretching vibrations couple to the ν_{as}(C≡C) and ν_s(C≡C) modes and four ν(C≡C) modes are observed: two asymmetric (IR active) and two symmetric (Raman active) (Table 3). These splitted ν(C≡C) modes were omitted in further analysis. These examples reveal that the spectral picture in which two ν_{as}(C≡C) and

Table 3. IR and Raman Spectra Parameters of the ν_{as}(C≡C) and ν_s(C≡C) Bands (Frequencies in cm^{-1}, IR Intensities in km mol^{-1}, Raman Activities in A^4 amu^{-1}, ρ(.) Depolarization Ratio, $\Delta\nu = \nu_s$(C≡C)-ν_{as}(C≡C)) of Symmetrically Disubstituted Diacetylenes Calculated at the B3LYP/aug-cc-pVDZ Level[b]

	asymmetric stretching				symmetric stretching				
substituent	$\nu_{as}(C\equiv C)_{sc}$	I_{IR}	A_R	$\rho(\nu_{as})$	$\nu_s(C\equiv C)_{sc}$	I_{IR}	A_R	$\rho(\nu_s)$	$\Delta\nu$
Li	1942	254.82	0.00	0.248	2093	0.00	4297	0.236	151
MgH	1997	275.62	0.00	0.335	2143	0.00	3556	0.271	146
Na	1933	85.55	0.00	0.180	2087	0.00	3701	0.208	154
BeH	2032	108.77	0.00	0.282	2182	0.00	3131	0.266	150
$SiMe_3$	2071	202.89	0.01	0.750	2198	0.00	6326	0.302	127
SiH_3	2082	27.26	242.7	0.145	2207	0.00	4001	0.327	124
BF_2	2129	484.40	0.04	0.750	2229	0.00	2509	0.301	100
$MeSO_2$	2112	220.49	0.03	0.750	2228	0.02	5794	0.312	116
BH_2	2042	225.09	0.02	0.714	2064	0.00	4961	0.301	22
H	2021	5.43	0.00	0.000	2190	0.00	1015	0.243	168
MeSO	2080	93.62	3.56	0.750	2188	0.01	8706	0.318	109
SO_2F	2132	231.52	0.19	0.748	2238	0.10	5045	0.313	106
MeS	2068	21.35	6.15	0.736	2130	2.09	9518	0.318	62
SH	2089	19.53	1.62	0.749	2159	1.32	6044	0.315	70
$COCH_3$	2130	233.31	0.56	0.693	2216	0.36	5174	0.313	86
Br	2124	63.81	0.00	0.311	2233	0.00	4477	0.319	109
CF_3	2198	212.43	0.00	0.300	2300	0.00	2123	0.296	102
CFO	2163	310.76	2.22	0.750	2237	0.02	4217	0.311	74
COOH	2161	277.16	0.96	0.750	2243	0.38	4660	0.311	82
$CONH_2$	2151	186.80	0.48	0.750	2245	0.62	5067	0.308	95
CHO	2130	250.28	2.63	0.750	2214	0.00	4088	0.309	84
CN [a]	2091	0.21	0.00	0.493	2189	0.00	9	0.577	-
	2264	66.40	0.00	0.700	2230	0.00	10257	0.317	-
Cl	2152	116.46	0.00	0.291	2257	0.00	3002	0.310	105
CH_3	2173	2.86	0.00	0.450	2276	0.00	2659	0.292	103
$CHCH_2(C_{2v})$	2141	8.34	43.38	0.750	2216	0.01	12410	0.320	75
$CHCH_2(C_{2v})$	2141	8.48	0.00	0.734	2216	0.00	12996	0.319	75
Ph	2146	0.07	2.01	0.329	2225	0.00	38879	0.327	79
tBu	2155	1.91	0.00	0.749	2263	0.00	4754	0.295	109
COCN	2141	417.16	0.26	0.477	2220	0.05	7102	0.313	79
NMe_2	2152	447.63	1.32	0.750	2186	0.17	5832	0.298	34
NH_2	2178	273.63	0.60	0.750	2220	0.03	2584	0.298	43
NO_2	2166	134.94	0.05	0.750	2225	0.00	6726	0.320	58
NO [a]	1525	952.08	0.00	0.000	2140	0.00	1751	0.324	-
	2330	2006.0	0.00	0.304	2318	0.00	2470	0.308	-
OH	2222	377.36	0.86	0.750	2308	0.34	1257	0.269	86
COOMe	2212	390.71	8.86	0.750	2300	0.20	4548	0.298	88
OCN[a]	2253	4.21	0.00	0.294	2290	0.00	6763	0.292	-
	2327	4241.4	0.00	0.324	2387	0.00	2088	0.318	-
F	2273	375.60	0.00	0.000	2373	0.00	666	0.226	99

[a] The ν_{as}(C≡C) and ν_s(C≡C) cannot be distinguished because they couple with the substituent stretching vibrations. [b] Vibrational frequencies are scaled by a scaling factor of 0.960.

ν_s(C≡C) bands in substituted diacetylenes are affected only by substituent effect is sometimes oversimplified.

It is striking that the two mode frequencies are the highest for F and the lowest for Na/Li/BH_2 substituents. By correlating the ν(C≡C) band positions with the sEDA and pEDA descriptors (Table 1) a linear correlation of ν_{as}(C≡C) with sEDA (R = 0.866) and lack of such similar correlation with pEDA descriptor was found. Thus, the band position depends mainly on substituent σ electrons donation or withdrawal properties, i.e., depends on "substituent electronegativity". However, again the correlation with the (s+p)EDA descriptor is slightly stronger (R = 0.904, Figure 3a). Thus, the π electron effect slightly strengthens the correlation. For the ν_s(C≡C) mode also the correlation with sEDA is statistically meaningful (R = 0.701) but that with (s+p)EDA descriptor is a bit stronger (R = 0.728, Figure 3b). Notice, that the ν(C≡C) frequencies of the most stable

dx.doi.org/10.1021/ci1003587 |J. Chem. Inf. Model. 2011, 51, 283–295

Table 4. Juxtaposition of the Experimental and Scaled (0.960) Theoretical ν_{as}(C≡C) and ν_s(C≡C) Frequencies (cm^{-1}) for Some Symmetrically Disubstituted Diacetylenes Calculated at the B3LYP/aug-cc-pVDZ Level[a]

substituent	$\nu_{as}(C{\equiv}C)_{sc}$ [cm^{-1}]	$\nu_{as}(C{\equiv}C)_{exp}$ [cm^{-1}]	$\nu_s(C{\equiv}C)_{sc}$ [cm^{-1}]	$\nu_s(C{\equiv}C)_{exp}$ [cm^{-1}]	ref
Cu		2005		2175	64
Na	1933	1938 (monoNa)	2087	2138 (monoNa)	67
$SiMe_3$	2071	2080	2198		65
H	2021	2022.2	2190	2188.9	54
I		2094		2227	21
CN	2264	2266	2230	2235	19
	2091	2097	2189	2183	19
Br	2124	2127	2233	2207	19
CH_3	2173	2163	2276	2265	68
		2149 m		2266w; 2212 m	69
Ph	2146	2148	2225	2210	65,66
Cl	2152	2161	2257	2245	21

[a] w - weak; m - medium.

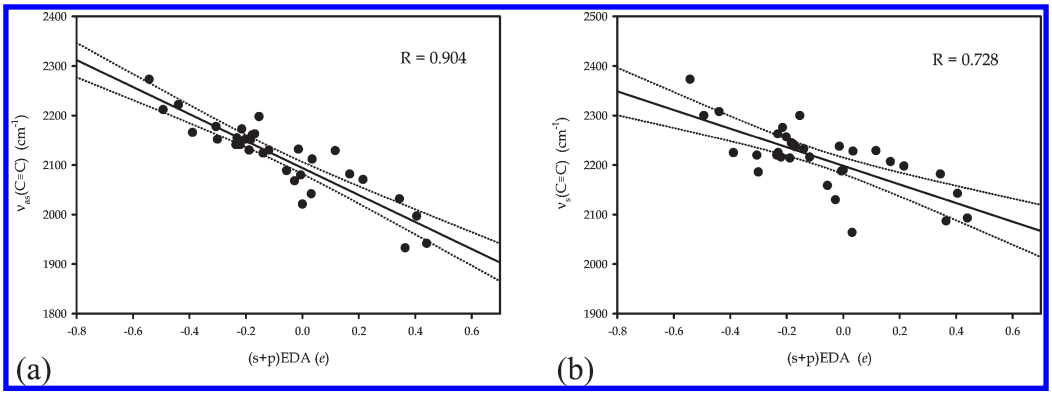

Figure 3. Linear regression between the B3LYP/aug-cc-pVDZ calculated ν_{as}(C≡C) (a) and ν_s(C≡C) (b) frequency of symmetrically disubstituted diacetylenes and (s+p)EDA descriptor. Dotted lines show the regression bands at the 95% confidence level.

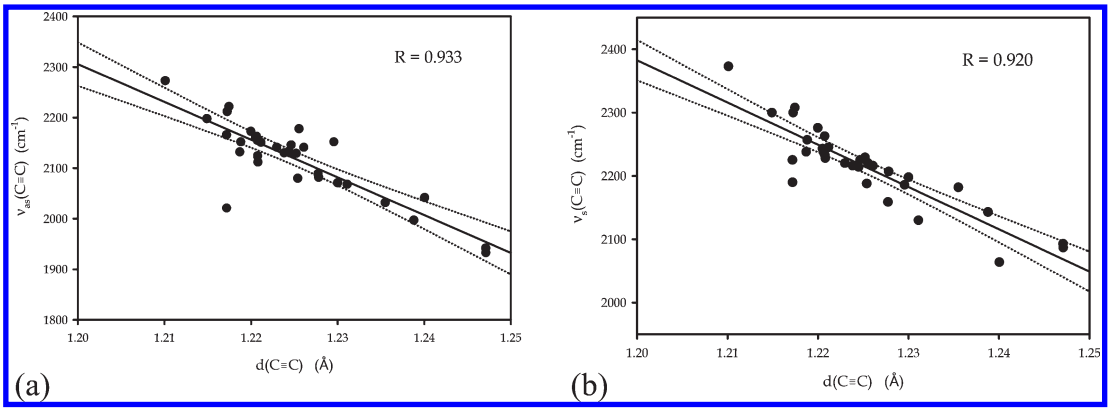

Figure 4. Linear regression between the B3LYP/aug-cc-pVDZ calculated ν_{as}(C≡C) (a) and ν_s(C≡C) (b) frequency of symmetrically disubstituted diacetylenes and triple bond length d(C≡C). Data for unsubstitutted diacetylene were excluded from correlations. Dotted lines show the regression bands at the 95% confidence level.

conformer were taken for analysis, but consideration of the other conformers is statistically insignificant for correlation analysis.

Both, the triple bond length and the ν_{as}(C≡C) and ν_s(C≡C) mode frequencies correlate with substituent effect (s+p)EDA descriptor; therefore, it is not surprising that these values are mutually intercorrelated with the correlation coefficient R = 0.933 and 0.920, respectively (Figure 4). A weak linear tendency between the ν(C≡C) band splitting and the single bond length can also be observed (R = 0.766).

3.3.4. The ν(C≡C) Mode IR and Raman Intensities. The B3LYP/cc-pVDZ calculated ν_{as}(C≡C) band IR intensities and the ν_s(C≡C) band Raman activities vary as the substituents are changed (Table 3). The ν_{as}(C≡C) IR intensity changes from 0.07 km mol^{-1} for diphenyldiacetylene, through 2.9 km mol^{-1}

dx.doi.org/10.1021/ci1003587 |J. Chem. Inf. Model. 2011, 51, 283–295

Table 5. Chemical Shifts (ppm) of Carbon Atoms and J-Coupling Constants (Hz) between Carbon Atoms in Symmetrically Disubstituted Diacetylenes (X-C1≡C2−C3≡C4-X) Calculated at the B3LYP/aug-cc-pVDZ-su1 Level

substituent X	δ(C1,C4) [ppm]	δ(C2,C3) [ppm]	$^1J_{C1-C2}$ [Hz]	$^1J_{C2-C3}$ [Hz]	$^2J_{C1-C3}$ [Hz]	$^3J_{C1-C4}$ [Hz]
Li	98.2	88.8	99.42	126.99	3.97	14.52
MgH	86.2	87.0	120.99	136.85	6.71	15.95
Na	90.5	92.2	90.17	124.81	1.56	15.73
BeH	88.4	80.8	141.34	146.49	9.83	16.13
$SiMe_3$	80.8	85.2	161.00	151.61	11.38	18.19
$SiEt_3$ exp.[122]	82.65	90.1	146.42	137.23	12.98	14.11
SiH_3	71.8	87.2	170.68	155.44	12.26	18.79
BF_2	75.5	83.7	183.14	161.97	14.38	17.86
$MeSO_2$	80.3	65.6	206.60	172.18	13.16	22.54
BH_2	127.1	125.9	161.28	160.57	13.28	14.92
H	56.3	63.5	213.44	169.63	18.10	19.61
H[a]			222.26	171.22		
H exp.[122]	65.18	67.60	194.1	154.9	18.9	16.0
MeSO	88.3	79.6	192.27	168.59	11.82	21.90
SO_2F	72.5	65.3	229.54	179.22	15.16	23.36
MeS	77.5	79.2	216.71	176.67	18.94	19.62
SH	64.7	75.8	224.05	177.70	19.12	20.81
$COCH_3$	81.0	70.4	200.32	170.64	14.51	19.66
Br	53.0	60.6	250.54	184.01	20.91	23.30
CF_3	65.4	65.3	229.05	176.84	17.80	21.22
CFO	69.4	71.4	222.93	177.40	16.94	20.37
COOH	71.3	69.9	217.81	174.85	16.77	20.25
$CONH_2$	71.9	65.8	208.76	171.73	16.14	19.88
CHO	83.4	74.5	201.33	171.79	14.02	19.70
CN	47.5	58.3	243.21	185.71	17.51	22.16
Cl	54.0	49.6	266.81	189.81	23.45	22.63
CH_3	66.7	61.9	211.65	170.70	18.90	19.37
$CHCH_2$ (C_{2v})	79.1	75.8	211.81	174.36	16.74	20.21
$CHCH_2$ (C_{2h})	79.1	75.7	212.00	174.59	16.87	20.25
Ph	81.9	75.7	211.28	173.15	18.05	19.26
tBu	82.9	63.1	202.42	168.53	17.58	18.87
COCN	83.7	75.4	212.71	176.55	14.90	20.05
NMe_2	85.4	54.9	243.29	188.32	26.17	15.98
NH_2	74.6	50.9	248.85	188.19	26.46	17.32
NO_2	80.4	50.3	259.02	191.80	19.30	22.21
NO	27.7	45.6	233.76	257.03	24.06	12.48
OH	77.2	25.5	276.57	197.69	28.67	19.22
COOMe	78.2	38.5	277.85	197.74	28.25	19.00
OCF3	71.7	34.2	290.03	200.05	28.47	20.13
OCN	64.8	17.0	326.67	212.05	33.33	20.07
F	80.7	11.2	316.93	210.31	31.97	20.68

[a] B3LYP/(11s,7p,2d/6s,2p)[7s,6p,2d/4s,2p].[83]

for dimethyldiacetylene, 5.4 km mol^{-1} for unsubstituted diacetylene, ca. 63 km mol^{-1} for dibromodiacetylene, ca. 116 km mol^{-1} for dichlorodiacetylene, ca. 250 km mol^{-1} for dilithiumdiacetylene, ca. 375 km mol^{-1} for difluorodiacetylene, to over 400 km mol^{-1} for dicyanocarboxy- and dimethylaminodiacetylene. The changeability of the Raman ν_s(C≡C) band Raman activities is great as well: from ca. 700 A^4 amu^{-1} for difluorodiacetylene, through ca. 6700 A^4 amu^{-1} for dinitrodiacetylene, to ca. 39 000 A^4 amu^{-1} for diphenyldiacetylene. Despite such a large intensity variations, correlation neither with substituent parameters nor with geometrical data was observed. This is even more true for the ν_{as}(C≡C) band Raman activities and the ν_s(C≡C) IR band intensities, which are inactive for molecules with center of symmetry and becomes slightly active when this symmetry is broken.

3.4. ^{13}C NMR Spectra of Diacetylenes. Symmetrically disubstituted diacetylenes belong to the AA'BB'-type system, and its ^{13}C NMR spectrum is determined by six independent parameters: δ(A)=δ(C1)=δ(C4), δ(B)=δ(C2)=δ(C3), J(AA')=^{3}J(C1C4), J(BB')=^{1}J(C2C3), J(AB)=^{1}J(C1C2)=^{1}J(C4C3), and J(A'B)=^{2}J(C4C2)=^{2}J(C1C3) yielding the ^{13}C NMR spectral pattern of 24 signals irresolvable experimentally

dx.doi.org/10.1021/ci1003587 |J. Chem. Inf. Model. 2011, 51, 283–295

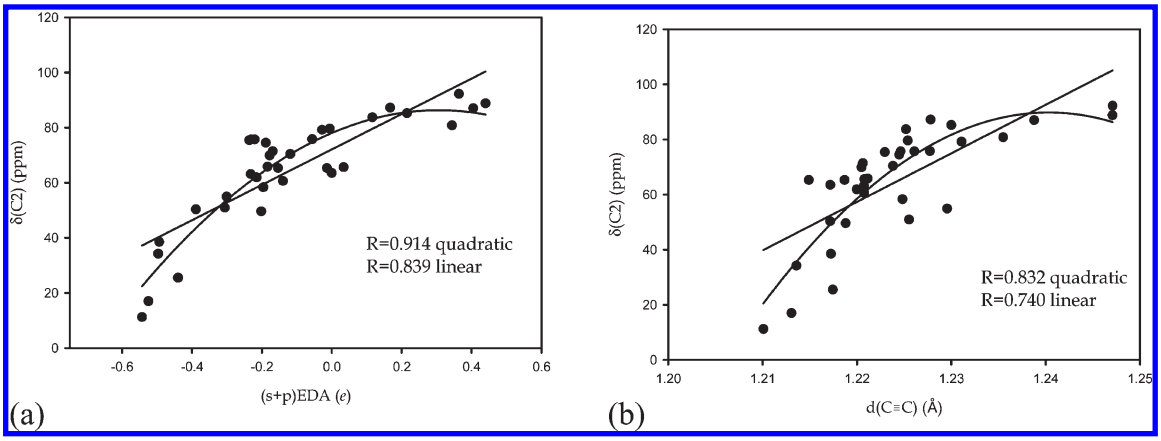

Figure 5. Change of the B3LYP/aug-cc-pVDZ-su1 calculated C2 chemical shifts with change of the (s+p)EDA substituent parameter (a) d(C≡C) triple bond length (b). Values for the BH_2 substituent were ignored.

without full ^{13}C substitution of the moiety and computer simulations of knotty coupling pattern.[70,71] In 1980 Kamieńska-Trela determined the complete set of $^{13}C-^{13}C$ spin−spin coupling constants (SSCC) in the fully ^{13}C enriched diacetylene (Table 5) and its bis(triethylsilyl) derivative.[70] Earlier, $^{1}J(C\equiv C)$ has been determined for ditert-butyldiacetylene and bis-(trimethyl)stannyldiacetylene by Hölzl and Wrackmeyer.[72] The SSCC in a series of mono- and disubstituted diacetylenes measured and calculated by the INDO semiempirical method by Kamieńska-Trela group[73−75] have shown that the $^{1}J(C\equiv C)$ and $^{1}J(C-C)$ INDO SSCC correlate with the Pauling's electronegativity of the first atom of the substituents.[75] On the other hand, already in the 1960s it was shown that ^{19}F NMR chemical shifts of *m*-substituted fluorobenzenes can estimate field inductive effects[76] and that ^{13}C NMR chemical shift of substituted styrenes can serve as a new σ scale for para substituents.[77] Thus, below we check whether the calculated ^{13}C NMR parameters of the diacetylene system follow changes in substituent descriptors or not.

3.4.1. Chemical Shifts. The experimental ^{13}C NMR chemical shifts of diacetylenes fall into the interval of 60−90 ppm.[75] The B3LYP/aug-cc-pVDZ-su1 calculated values show that upon change of the substituent the δ(C1) can possibly vary from ca. 50 to 130 ppm, whereas the δ(C2) can vary even more: from ca. 10 to 125 ppm (Table 5). However, some values are surprising and rather exceptional: δ > 100 ppm is calculated only for the BH_2 substituent, whereas δ(C1) near 25 ppm is predicted only for NO substituent with strong electronic conjugations, whereas δ(C1) is near 50 ppm also for the electron conjugated CN substituent. On the other hand, despite the δ(C2) values are more differentiated, they change more systematically: for a group of strongly σ-electron withdrawing substituents they decrease from ca. 50 toward ca. 10 ppm (bottom of Table 5). Surprisingly, only the δ(C2) chemical shift does correlate with sEDA (and a bit better) with (s+p)EDA descriptor, yet, a quadratic rather than linear correlation seems to be adequate (Figure 5a). The same holds true for correlation of δ(C2) with d(C≡C) (Figure 5b). Thus, the electron distribution around the C2 atom is more sensitive to the substituent effect than that around C1 atom. Also, the diamagnetic contribution to the shielding constant propagating through the σ-electrons is substantially responsible for the effect. In contrast to the chemical intuition, the δ(C2) deshielding increases when the electron donating properties are increased and d(C≡C) is increased. This is another manifestation of the phenomenon discussed in the *Geometry* section: the σ-electron repulsion in the space of C≡C bonds seems to be responsible for an increase of the bond, so when the electrons are supplied to the diacetylene system the bond is elongated and C2 nuclei is deshielded.

3.4.2. J(CC) Shielding Constants. The $^{1}J(CC)$ carbon−carbon SSCCs reflect electron distribution within the most important bonds for organic chemistry;[78] however, it took some time until it was recognized that hybridization of the C-atoms involved and electronegativity of the substituents attached to a given bond are the main factors which govern $^{1}J(CC)$.[79] The long-range $^{n}J(CC)$'s (n > 1) depend also upon the path across which the coupling occurs. It has been demonstrated that the substituent effect is strictly localized and primarily limited to the closest CC bond.[80] In acetylenes, the $^{1}J(C\equiv C)$ magnitude ranges from ca. 55 Hz ($Et_3SiC\equiv CLi$) to ca. 230 Hz (m-MeO-$C_6H_4O-C\equiv CMe$), whereas theoretical calculations predict the range to be much larger: from 30 Hz (Li_2C_2) to ca. 400 Hz (F_2C_2).[81,82] Recently, the $^{1}J(C\equiv C)$s in RC≡CH has been shown to display anomalously high sensitivity to solvent due to C−H...B H-bond formation (ca. 13 Hz).[78]

In 1999, Kamieńska-Trela et al. observed and successfully calculated the $^{1}J(CC)$ SSCC in substituted diacetylenes.[75] They found these $^{1}J(CC)$'s to be "one of the most sensitive measure of the electronic structure of the carbon−carbon bond" and show the substituent influence to be not transferred along the conjugated triple bond system. The $^{1}J(C\equiv C)$ has been as small as 62.5 Hz for the Li- and as large as 226.8 Hz for the F-substituted compound covering range of ca. 165 Hz. Due to necessity to synthesize ^{13}C-enriched diacetylenes to register the $^{1}J(C-C)$'s only a limited number of values is known, and they fall into the 154-162 Hz range.[70,71,73,75,79] The couplings across the single C−C bonds are entirely governed by the Fermi contact (FC) contribution, whereas for the couplings across the triple C≡C bonds the FC is dominating, yet, the orbital-dipol (OD) and spin-dipol (SD) sum usually accounts for ca. 10% of the total $^{1}J(C\equiv C)$. This is also true for diacetylene $^{1}J(CC)$'s calculated at the B3LYP/(11s,7p,2d/6s,2p) [7s,6p,2d/4s,2p] level.[83]

The B3LYP/aug-cc-pVDZ-su1 calculated coupling constants through one, two, and three bonds of symmetrically substituted diacetylene systems (Table 5) demonstrate the $^{1}J(C1\equiv C2)$, $^{1}J(C2-C3)$, $^{2}J(C1\equiv C-C3)$, and $^{4}J(C1\equiv C-C\equiv C4)$ to fall in the range of 90−320 Hz, 120−260 Hz, 4−34 Hz, and 14−24 Hz, respectively. For diacetylene the predicted $^{1}J(C1\equiv C2)$ and

dx.doi.org/10.1021/ci1003587 |*J. Chem. Inf. Model.* 2011, 51, 283–295

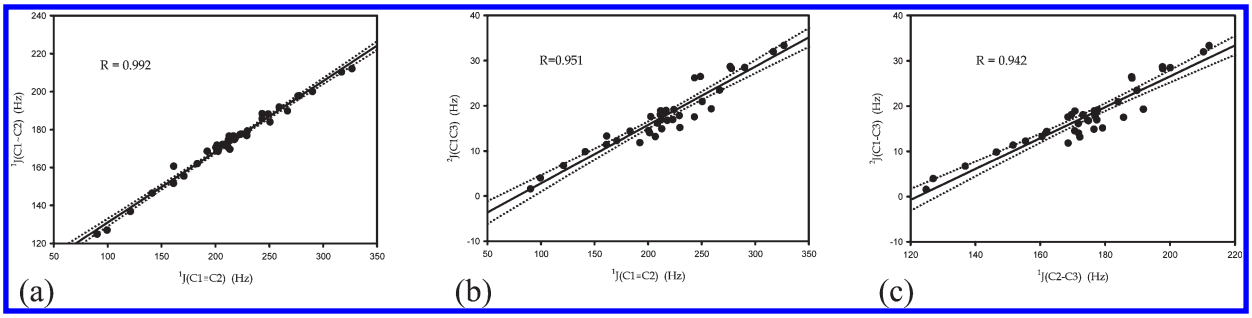

Figure 6. Mutual correlations between the B3LYP/aug-cc-pVDZ-su1 calculated ^{1}J(C≡C) and ^{1}J(C−C) (a) and ^{1}J(C≡C) and ^{2}J(C−C) (b) and ^{1}J(C−C) and ^{2}J(C−C) (c) coupling constants in symmetrically substituted diacetylenes. Dotted lines show the regression bands at the 95% confidence level.

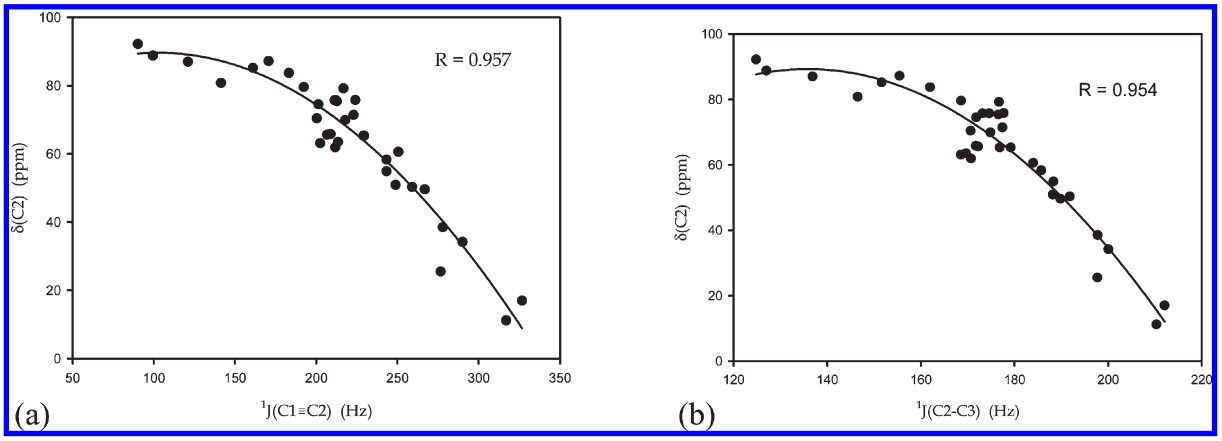

Figure 7. Correlations between δ(C2) chemical shift and ^{1}J(C1≡C2) (a) and ^{1}J(C2−C3) (b) coupling constants in substituted diacetylenes.

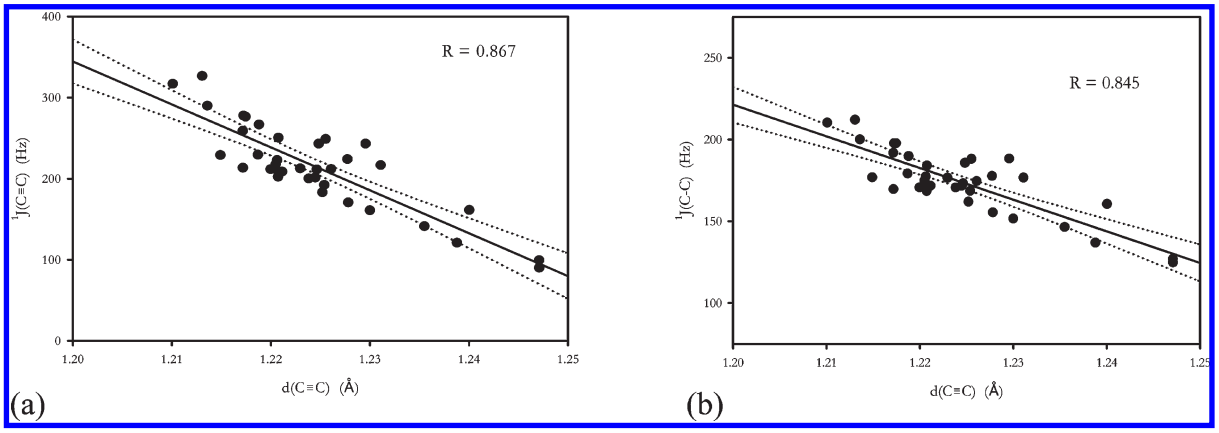

Figure 8. Decrease of the B3LYP/aug-cc-pVDZ-su1 calculated ^{1}J(C≡C) (a) and ^{1}J(C−C) (b) coupling constants with an increase of the d(C≡C) bond length. Dotted lines show the regression bands at the 95% confidence level.

^{1}J(C2−C3) values are ca. 10% higher than the experimental ones: 213 vs 194 Hz and 170 vs 155 Hz, respectively, while for ^{2}J(C1C3) and ^{4}J(C1C4) the agreement is as follows: 18.1 vs 18.9, and 19.6 vs 16.0, respectively. The ^{1}J(C1≡C2) and ^{1}J(C2−C3) are mutually correlated as well as ^{1}J(C1≡C2) and ^{1}J(C2−C3) with ^{2}J(C1C3) (Figure 6a-c). The coupling through three bonds is practically not correlated with the above three J(CC)'s.

Interestingly, there are correlations between δ(C2) chemical shift and ^{1}J(C1≡C2) and ^{1}J(C2−C3) coupling constants showing an increase of shielding (upfield shift) as the ^{1}J(CC)'s are increased (Figure 7), which means that an increase in electron density at the C2 nuclei is correlated with an increase of the coupling constants.

Note, that the calculated ^{1}J(CC) SSCCs decrease with an increase of the triple bond length (Figure 8). It is simple why the ^{1}J(C1≡C2) coupling is decreasing with an increase of the C1≡C2 bond length through which the interaction occurs, but why it is so for ^{1}J(C2−C3) interacting through the single bond is not so clear. In diacetylenes the Fermi contact is responsible for the ^{1}J(C2−C3) coupling,[75,83] and the FC term probes the spin polarization of the *s* electrons only (density of electrons with higher angular momentum at the nuclei approaches zero). Increase of the C1≡C2 and C3≡C2 bond lengths density of *s*

dx.doi.org/10.1021/ci1003587 |*J. Chem. Inf. Model.* 2011, 51, 283–295

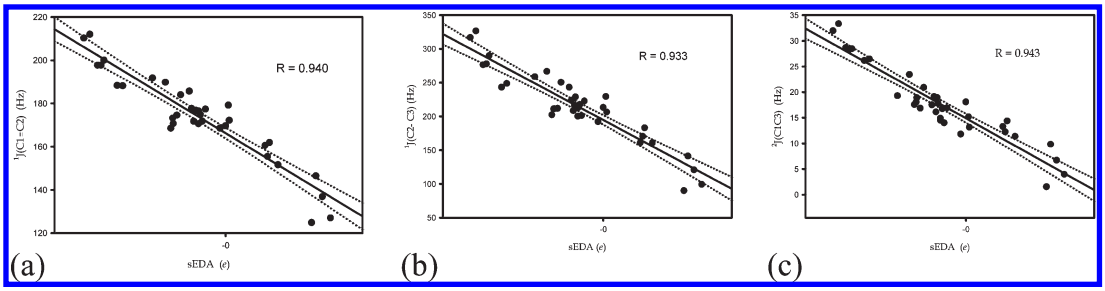

Figure 9. Decrease of the B3LYP/aug-cc-pVDZ-su1 calculated $^{1}J(C{\equiv}C)$ (a), $^{1}J(C{-}C)$ (b), and $^{2}J(C1C3)$ (c) coupling constants with an increase of the sEDA substituent parameter. Dotted lines show the regression bands at the 95% confidence level.

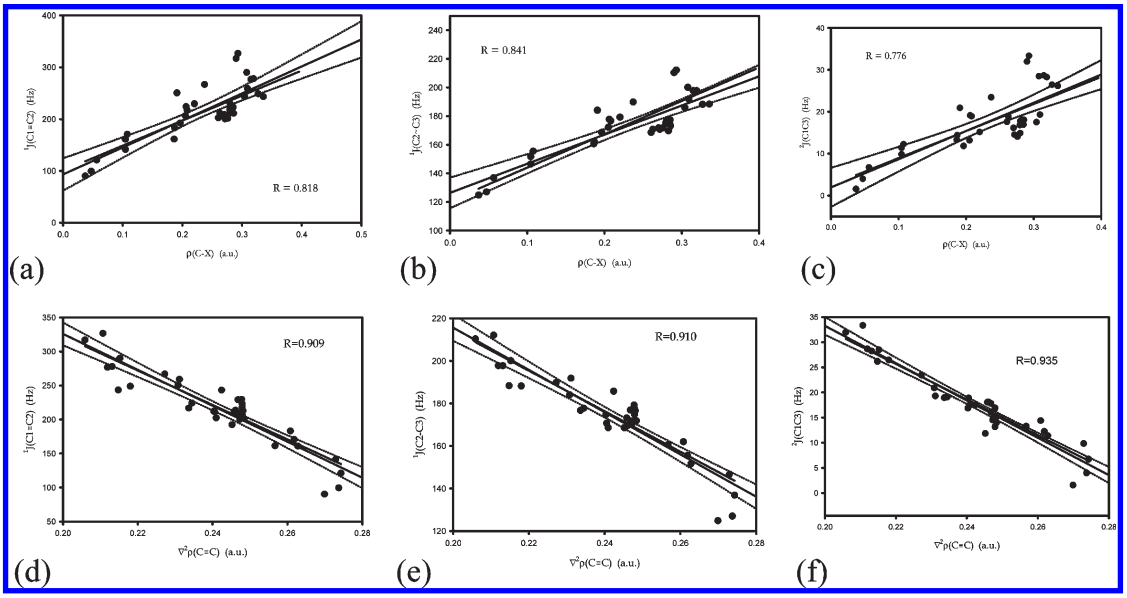

Figure 10. The $^{1}J(C1{\equiv}C2)$, $^{1}J(C2{-}C3)$, and $^{2}J(C1C3)$ increase with the $\rho(CX)$ electron density (a), (b), and (c), respectively, and the decrease of the $^{1}J(C1{\equiv}C2)$, $^{1}J(C2{-}C3)$, and $^{2}J(C1C3)$ with the $\nabla^{2}\rho(C1{\equiv}C2)$ Laplacian of electron density in the triple bond BCP. Dotted lines show the regression bands at the 95% confidence level.

electrons at C2 and C3 decrease and the FC term decrease as well, and the $^{1}J(C2{-}C3)$ coupling follows this term. The other question arises: why the analogous dependence of $^{1}J(C2{-}C3)$ on d(C2−C3) does not occur. This is because the change in C1≡C2 distance influences more the size of the diacetylene moiety than the C2−C3 distance does.

Let us to stress now that an increase of the sEDA parameter means a decrease of the group electronegativity. Thus, the decrease of the calculated $^{1}J(CC)$ coupling constants with an increase of the sEDA parameter (Figure 9a,b) is qualitatively the same observation that the Kamieńska-Trela et al. reports on an increase of $^{1}J(CC)$'s with Pauling electronegativity of the first atoms in substituents.[75] Moreover, we can show that $^{2}J(C1C3)$ follows the same tendency (Figure 9c), whereas the $^{4}J(C1C4)$ coupling behaves more chaotically.

Additional trends can be found between bond critical point parameters and the coupling constants (Figure 10). The $^{1}J(C1{\equiv}C2)$, $^{1}J(C2{-}C3)$, and $^{2}J(C1C3)$ increase as the $\rho(CX)$ electron density in the CX BCP is increased, and they decrease as the $\nabla^{2}\rho(C1{\equiv}C2)$ Laplacian of electron density in the triple bond BCP is increased. The first three tendencies (Figure 10a-c) demonstrate yet another variation of the fact that $\rho(C\text{-}X)$ tends to increase with the increasing overall electron donating properties of the substituent: the electron density is pushed by a substituent more and more off the X-C bond to the diacetylene system and the J(CC)'s increase. The second three tendencies (Figure 10d-f) show that the three J(CC)'s decrease as the electron density in the C≡C BCP is reduced.

4. CONCLUSIONS

Symmetrically disubstituted diacetylenes were studied by means of the B3LYP/aug-cc-pVDZ calculations. Based on data collected for over 35 substituted diacetylenes, the substituent effect on C≡C and C−C bond lengths electron density properties in bond critical points, theoretical vibrational frequencies and IR and Raman intensities, and ^{13}C NMR chemical shifts and coupling constants were analyzed by using the sEDA and pEDA substituent effect descriptors. It is demonstrated that, surprisingly, the triple bond length increases with the electron donating and decreases with the electron withdrawing properties of the substituents. This unexpected tendency is probably connected with the σ-electron repulsion in the space of C≡C. A linear decrease of charge density $\rho(C\text{-}X)$ with an increase of sEDA is found indicating that $\rho(C\text{-}X)$ tends to decrease with the increasing σ-electron donating properties of the substituent. This means that the electron density is pushed off the X-C bond to the diacetylene system. There is a linear correlation between $\nabla^{2}\rho(C{\equiv}C)$ and

dx.doi.org/10.1021/ci1003587 |J. Chem. Inf. Model. 2011, 51, 283–295

(s+p)EDA which is clear and means that ρ(C≡C) is depleting with the increasing of the overall electron donating properties of the substituent. It is demonstrated that the ν_{as}(C≡C) and ν_{s}(C≡C) mode frequencies decrease with the electron donating and increase with the electron withdrawing properties of the substituents. The effect is due to the σ-electron donor−acceptor properties of the substituents; however, the linear correlations are a bit improved when an influence on both σ-and π-valence electrons is considered. Surprisingly, the calculated chemical shift of the C1-atom δ(C1) does not correlate with the substituent descriptors, whereas the δ(C2) does correlate with sEDA and also with d(C≡C). The B3LYP/aug-cc-pVDZ-su1 calculated coupling constants demonstrate that there are correlations between the δ(C2) chemical shift and ^{1}J(C1≡C2) and ^{1}J(C2−C3) coupling constants showing an upfield shift as the ^{1}J(CC)'s are increased. The calculated ^{1}J(CC) coupling constants decrease with an increase of the triple bond length. The decrease of the calculated ^{1}J(CC) coupling constants with an increase of the sEDA parameter is also shown and confirms the Kamieńska-Trela et al. earlier reports. The ^{1}J(C1≡C2), ^{1}J(C2−C3), and ^{2}J(C1C3) are also shown to increase as the ρ(CX) electron density in the CX BCP is increased, and they decrease as the $\nabla^{2}\rho$(C1≡C2) Laplacian of electron density in the triple bond BCP is increased.

■ ASSOCIATED CONTENT

Supporting Information. Tables with total energies and Gibbs energies values of the studied compounds; selected parameters in bond critical points calculated by the AIM method; juxtaposition of the sEDA, pEDA, and (s+p)EDA descriptors and the NBO determined sum of the σ and π valence orbital occupancies and total number of valence electrons in diacetylene moiety; vibrational ν_{as}(C≡C) and ν_{s}(C≡C) bands parameters and C≡C and C−C bond lengths calculated at the B3LYP/cc-pVDZ level. This material is available free of charge via the Internet at http://pubs.acs.org.

■ AUTHOR INFORMATION

Corresponding Author

*Phone: +48 12 6632253. Fax: +48 12 6340515. E-mail: baranska@chemia.uj.edu.pl.

■ ACKNOWLEDGMENT

The authors thank for the computing time to the Academic Computer Centre CYFRONET AGH, Kraków, Poland. The computational grants G18-4 and G19-4 from the Interdisciplinary Center of Mathematical and Computer Modeling (ICM) at Warsaw University are gratefully acknowledged. The research was supported by the Ministry of Science and Higher Education (MNiSW, grant No. N204013635, 2008-2011). International PhD-studies programme at the Faculty of Chemistry Jagiellonian University within the Foundation for Polish Science MPD Programme is also kindly acknowledged (M.R.).

■ REFERENCES

(1) Glaser, C. Beiträge zur Kenntniss des Acetenylbenzols. *Ber. Dtsch. Chem. Ges.* **1869**, *2*, 422–424.

(2) Sun, Y.; Taylor, N. J.; Carty, A. J. Models for Linear Acetylide Polymers: Synthesis and Single-Crystal X-ray Structures of the Ruthenium(II) Acetylide and Dlacetylldes $Ru(CO)_2(PEt_3)_2$ $[(C{=}C)_nR]_2$, n= 1, R =Me,Si; n = 2, R = Me,Si, H). *Organometallics* **1992**, *1 I*, 4293–4300.

(3) Volkov, A. N.; Volkova, K. A. α-Haloacetylene and diacetylene alcohols. *Russ. J. Org. Chem.* **2007**, *43*, 161–169.

(4) Shirakawa, H.; Louis, E. J.; MacDiarmid, A. G.; Chiang, C. K.; Heeger, A. J. Synthesis of Electrically Conducting Organic Polymers: Halogen Derivatives of Polyacetylene, $(CH)_x$. *J. Chem. Soc., Chem. Commun.* **1977**, *16*, 578–580.

(5) Hall, N. Twenty-five years of conducting polymers. *Chem. Commun.* **2003**, *9*, 1–4.

(6) Sun, A.; Lauher, J. W.; Goroff, N. S. Preparation of poly(diiododiacetylene), an ordered conjugated polymer of carbon and iodine. *Science* **2006**, *312*, 1030–1034.

(7) Bohlmann, F.; Bronowski, H.; Arndt, Ch. Natürlisch vorkommende Acetylenverbindungen. *Fortschr. Chem. Forsch.* **1962**, *4*, 138–272.

(8) Bohlmann, F. Natürlisch vorkommende Acetylen-verbindungen. *Fortschr. Chem. Forsch.* **1965**, *6*, 65–100.

(9) Hansen, L.; Boll, P. M. Polyacetylenes in Araliaceae: Their chemistry, biosynthesis and biological significance. *Phytochemistry* **1986**, *25*, 285–293.

(10) Baranski, R.; Baranska, M.; Schulz, H.; Simon, P. W.; Nothnagel, T. Single seed Raman measurements allow taxonomical discrimination of Apiaceae Accesions collected in Gene Banks. *Biopolymers* **2006**, *81*, 497–505.

(11) Hansen, S. L.; Purup, S.; Christensen, L. P. Bioactivity of falcarinol and the influence of processing and storage on its content in carrots (*Daucus carota* L). *J. Sci. Food Agric.* **2003**, *83*, 1010–1017.

(12) Baranska, M.; Schulz, H. Spatial tissue distribution of polyacetylenes in carrot root. *Analyst* **2005**, *130*, 855–859.

(13) Baranska, M.; Schulz, H.; Baranski, R.; Nothnagel, T.; Christensen, L. P. In Situ Simultaneous Analysis of Polyacetylenes, Carotenoids and Polysaccharides in Carrot Roots. *J. Agric. Food Chem.* **2005**, *53*, 6565–6571.

(14) Baranska, M.; Schulz, H.; Christensen, L. P. Structural Changes of Polyacetylenes in American Ginseng Root Can Be Observed in Situ by Using Raman Spectroscopy. *J. Agric. Food Chem.* **2006**, *54*, 3629–3635.

(15) Ziurys, L. M. The chemistry in circumstellar envelopes of evolved stars: Following the origin of the elements to the origin of life. *Proc. Natl. Acad. Sci.* **2006**, *103*, 12274–12279.

(16) Walmsley, C. M.; Winnewisser, G.; Toelle, F. Cyanoacetylene and cyanodiacetylene in interstellar clouds. *A&A* **1980**, *81*, 245–250.

(17) Coupeaud, A.; Turowski, M.; Gronowski, M.; Pietri, N.; Couturier-Tamburelli, I.; Kolos, R.; Aycard, J. P. Spectroscopy of cyanodiacetylene in solid argon and the generation of isocyano diacetylene. *J. Chem. Phys.* **2007**, *126*, 164301–164308.

(18) Miller, F. A.; Lemmon, D. H. The infrared and Raman spectra of dicyanodiacetylene, NCCCCCCN. *Spectrochim. Acta* **1967**, *23A*, 1415–1423.

(19) Kolos, R. Photolysis of dicyanodiacetylene in argon matrices. *Chem. Phys. Lett.* **1999**, *299*, 247–251.

(20) Bayer, A. Ueber polyacatylenverbindungen. *Ber. Dtsch. Chem. Ges.* **1885**, *18*, 2269–2281.

(21) Klaboe, P.; Kloster-Jensen, E.; Bjarnov, E.; Christiensen, D. H.; Nielsen, O. F. The vibrational spectra and force fields of dichloro-, dibromo- and diiododiacetylene. *Spectrochim. Acta* **1975**, *31A*, 931–943.

(22) Pfau, A. S.; Pictet, J.; Plattner, P.; Susz, B. Etudes sur les matières végétales volatiles III. Constitution et synthèse du Carlinoxyde. *Helv. Chim. Acta* **1935**, *18*, 935–951.

(23) Schrader, B.; Schulz, H.; Baranska, M.; Andreev, G. N.; Lehner, C.; Sawatzki, J. Non-destructive Raman analyses − polyacetylenes in plants. *Spectrochim. Acta* **2005**, *61A*, 1395–1401.

(24) Schulz, H.; Baranska, M. Identification and quantification of valuable plant substances by IR and Raman spectroscopy. *Vib. Spectrosc.* **2007**, *43*, 13–25.

(25) Even, J.; Bertault, M.; Girard, A.; Delugeard, Y.; Fave, J.-L. Dynamical study by Raman scattering of the ferroelectric phase transition of the disubstituted diacetylene 1,6-bis (2,4-dinitrophenoxy)-2, 4-hexadiyne (DNP). *Chem. Phys.* **1994**, *188*, 235–246.

(26) Taft, R. W.; Topsom, R. D. The Nature and Analysis of Substituent Effects. *Prog. Phys. Org. Chem.* **1987**, *16*, 1–83.
(27) Taft, R. W., Jr A Precise Correlation of Nuclear Magnetic Shielding in m- and p-Substituted Fluorobenzenes by Inductive and Resonance Parameters from Reactivity. *J. Am. Chem. Soc.* **1957**, *79*, 1045–1049.
(28) Hollingsworth, C. A.; Seybold, P. G.; Hadad, C. M. Substituent Effects on the Electronic Structure and pKa of Benzoic Acid. *Int. J. Quantum Chem.* **2002**, *90*, 1396–1403.
(29) Gross, K. C.; Seybold, P. G.; Hadad, C. M. Comparison of Different Atomic Charge Schemes for Predicting pKa Variations in Substituted Anilines and Phenols. *Int. J. Quantum Chem.* **2002**, *90*, 445–458.
(30) Sadlej-Sosnowska, N. On the Way to Physical Interpretation of Hammett Constants: How Substituent Active Space Impacts on Acidity and Electron Distribution in *p*-Substituted Benzoic Acid Molecules. *Pol. J. Chem.* **2007**, *81*, 1123–1134.
(31) Galabov, B.; Ilieva, S.; Schaefer, H. F., III An efficient computational approach for the evaluation of substituent constants. *J. Org. Chem.* **2006**, *71*, 6382–6387.
(32) Morao, I.; Hillier, I. H. Magnetic analysis (NICS) of monoarylic cations. Linear relationship between aromaticity and Hammett constants (σ_p^+). *Tetrahedron Lett.* **2001**, *42*, 4429–4431.
(33) Krygowski, T. M.; Stępień, B. T. Sigma- and Pi-electron delocalization: Focus on substituent effects. *Chem. Rev.* **2005**, *105*, 3482–3512.
(34) Oziminski, W. P. Tautomeria pięcioczłonowych pierścieni heterocyklicznych zawierających trzy heteroatomy. Badania obliczeniowe. Ph.D. Thesis, Institute of Nuclear Chemistry and Technology, Warsaw, 2008.
(35) Oziminski, W. P.; Dobrowolski, J. Cz. On the Substituent Effect. The Natural Population Analysis Approach. *J. Phys. Org. Chem.* **2009**, *22*, 769–778.
(36) Boyd, R. J.; Edgecombe, K. E. Atomic and group electronegativities from the electron-density distributions of molecules. *J. Am. Chem. Soc.* **1988**, *110*, 4182–4186.
(37) Boyd, R. J.; Boyd, S. L. Group electronegativities from the bond critical point model. *J. Am. Chem. Soc.* **1992**, *114*, 1652–1655.
(38) Marriott, S.; Reynolds, W. F.; Taft, R. W.; Topsom, R. D. Substituent electronegativity parameters. *J. Org. Chem.* **1984**, *49*, 959–965.
(39) Swain, C. G.; Lupton, E. C. Field and Resonance Components of Substituent Effects. *J. Am. Chem. Soc.* **1968**, *90*, 4328–4337.
(40) Becke, A. D. Density-functional thermochemistry. III. The role of exact exchange. *J. Chem. Phys.* **1993**, *98*, 5648–5652.
(41) Dunning, T. H., Jr. Gaussian basis sets for use in correlated molecular calculations. I. the atoms boron through neon and hydrogen. *J. Chem. Phys.* **1989**, *90*, 1007–1023.
(42) Kendall, R. A.; Dunning, T. H.; Harrison, R. J. Electron Affinities of the First-Row Atoms Revisited. Systematic Basis Sets and Wave Functions. *J. Chem. Phys.* **1992**, *96*, 6796–6806.
(43) Frisch, M. J.; Trucks, G. W.; Schlegel, H. B.; Scuseria, G. E.; Robb, M. A.; Cheeseman, J. R.; Scalmani, G.; Barone, V.; Mennucci, B.; Petersson, G. A.; Nakatsuji, H.; Caricato, M.; Li, X.; Hratchian, H. P.; Izmaylov, A. F.; Bloino, J.; Zheng, G.; Sonnenberg, J. L.; Hada, M.; Ehara, M.; Toyota, K.; Fukuda, R.; Hasegawa, J.; Ishida, M.; Nakajima, T.; Honda, Y.; Kitao, O.; Nakai, H.; Vreven, T.; Montgomery, Jr. J. A.; Peralta, J. E.; Ogliaro, F.; Bearpark, M.; Heyd, J. J.; Brothers, E.; Kudin, K. N.; Staroverov, V. N.; Kobayashi, R.; Normand, J.; Raghavachari, K.; Rendell, A.; Burant, J. C.; Iyengar, S. S.; Tomasi, J.; Cossi, M.; Rega, N.; Millam, J. M.; Klene, M.; Knox, J. E.; Cross, J. B.; Bakken, V.; Adamo, C.; Jaramillo, J.; Gomperts, R.; Stratmann, R. E.; Yazyev, O.; Austin, A. J.; Cammi, R.; Pomelli, C.; Ochterski, J. W.; Martin, R. L.; Morokuma, K.; Zakrzewski, V. G.; Voth, G. A.; Salvador, P.; Dannenberg, J. J.; Dapprich, S.; Daniels, A. D.; Farkas, O.; Foresman, J. B.; Ortiz, J. V.; Cioslowski, J.; Fox, D. J. *Gaussian 09, Revision A.1*; Gaussian Inc.: Wallingford, CT, 2009.
(44) Kevin, E.; Riley, K. E.; Op't Holt, B. T.; Merz, K. M., Jr. Critical Assessment of the Performance of Density Functional Methods for Several Atomic and Molecular Properties. *J. Chem. Theory Comput.* **2007**, *3*, 407–433.
(45) Popelier, P. L. A. *Atoms in molecules. An introduction*; 659 Prentice-Hall: Harlow, England, 2000.
(46) Biegler-König, F.; Schönbohm, J.; advices by Bader, R. F. W. AIM2000 A Program to Analyse and Visualize Atoms in Molecules Version 2. Büro für Innovative Software, C. Streibel Biegler-König Fröbelstrasse 68 33604 Bielefeld, Germany, 2002.
(47) Gauss, J. Effects of electron correlation in the calculation of nuclear magnetic resonance chemical shifts. *J. Chem. Phys.* **1993**, *99*, 3629–3643.
(48) Cheeseman, J. R.; Trucks, G. W.; Keith, T. A.; Frisch, M.J. A Comparison of Models for Calculating Nuclear-Magnetic-Resonance Shielding Tensors. *J. Chem. Phys.* **1996**, *104*, 5497–5509.
(49) Deng, W.; Cheeseman, J. R.; Frisch, M. J. Calculation of Nuclear Spin-Spin Coupling Constants of Molecules with First and Second Row Atoms in Study of Basis set Dependence. *J. Chem. Theory Comput.* **2006**, *2*, 1028–1037.
(50) Wolfram, K.; Holthausen, M. C. A In *Chemist's Guide to Density Functional Theory*, 2nd ed.; Wiley−VCH Verlag, GmbH: 2001; pp 212−215.
(51) Helgaker, T.; Jaszuński, M.; Ruud, K.; Górska, A. Basis-set dependence of nuclear spin-spin coupling constants. *Theor. Chim. Acc.* **1998**, *99*, 175–182.
(52) Cybulski, H.; Pecul, M.; Sadlej, J.; Helgaker, T. Characterization of dihydrogen-bonded D-H.H−A complexes on the basis of infrared and magnetic resonance spectroscopic parameters. *J. Chem. Phys.* **2003**, *119*, 5094–5104.
(53) Cybulski, H.; Tymińska, E.; Sadlej, J. The Properties of Weak and Strong Dihydrogen-Bonded D-H.H-A Complexes. *Chem. Phys. Chem.* **2006**, *7*, 629–639.
(54) Guelachvili, G.; Craig, A. M.; Ramsay, D. A. High-resolution Fourier studies of diacetylene in the regions of the ν_4 and ν_5 fundamentals. *J. Mol. Spectrosc.* **1984**, *105*, 156–192.
(55) Thorwirth, S.; Harding, M. E.; Muders, D.; Gauss, J. The empirical equilibrium structure of diacetylene. *J. Mol. Spectrosc.* **2008**, *251*, 220–223.
(56) Simmonett, A. C.; Schaefer, H. F., III; Allen, W. D. Enthalpy of formation and anharmonic force field of diacetylene. *J. Chem. Phys.* **2009**, *130*, 044301.
(57) Tay, R.; Metha, G. F.; Shanks, F.; McNaughton, D. Determination of the molecular structure of diacetylene from high-resolution FTIR spectroscopy. *Struct. Chem.* **1995**, *6*, 47–55.
(58) Meister, A. G.; Clevleland, F. F. The Non-degenerate vibrations of Dimethylacetylene, Diacetylene, and Dimethyldiacetylene. *J. Chem. Phys.* **1947**, *15*, 349–357.
(59) Fan, L.; Ziegler, T. Application of density functional theory to infrared absorption intensity calculations on main group molecules. *J. Chem. Phys.* **1992**, *96*, 9005–9012.
(60) Porezag, D.; Pederson, M. R. Infrared intensities and Raman-scattering activities within density-functional theory. *Phys. Rev.* **1996**, *54*, 7830–7836.
(61) Hippler, M. Quantum chemical study and infrared spectroscopy of hydrogen-bonded $CHCl_3$−NH_3 in the gas phase. *J. Chem. Phys.* **2007**, *127*, 084306.
(62) Perera, S. A.; Bartlett, R. J. Coupled-cluster calculations of Raman intensities and their application to N_4 and N_5^-. *Chem. Phys. Lett.* **1999**, *314*, 381–387.
(63) Jones, G. E.; Kendrick, D. A.; Holmes, A. B. Checked by Armstrong, J.; Heathcock, C. H. 1,4-Bis(Trimethylsilyl) Buta-1,3-Diyne [Silane, 1,3-butadiyne-1,4-diylbis [trimethyl-]]. *Org. Synth. Coll.* **1993**, *8*, 63; Vol. **1987**, 65, 52.
(64) Cataldo, F. Structural relationship between dicopper diacetylide (Cu-C≡C-C≡C-Cu) and dicopper acetylide (Cu-C≡C-Cu). *Eur. J. Solid State. Inorg. Chem.* **1998**, *35*, 281–291.
(65) Zimmermann, B.; Baranović, G. Two-dimensional infrared correlation spectroscopic study on thermal polymerization of diphenylbutadiyne. *Vib. Spectrosc.* **2006**, *41*, 126–135.

(66) Baranović, G.; Colombo, L.; Furic, K.; Durig, J. R.; Sullivan, J. F.; Mink, J. Vibrational assignment of 1,4-diphenylbutadiyne. *J. Mol. Struct.* **1986**, *144*, 53–69.

(67) Kanesaka, I.; Kawai, K. The i.r. spectrum of sodium diacetylide. *Spectrochim. Acta* **1976**, *32A*, 1443–1445.

(68) Nielsen, C. J. The vibrational spectra of 2,4-hexadiyne (dimethyldiacetylene), 2,4-hexadiyne-d6 and 2,4-hexadiyne-1,1,1-d3. *Spectrochim. Acta* **1983**, *39A*, 993–1005.

(69) Popov, E. M.; Lubuzh, E. D. Vibrational spectra of polyacetylenic compounds. *J. Appl. Spectrosc.* **1969**, *5*, 372–376.

(70) Kamieńska-Trela, K. ^{13}C-^{13}C Coupling constants in diacetylene (1,3-butadiyne) and its bis(triethylsilyl) derivative. *Org. Magn. Reson.* **1980**, *14*, 398–403.

(71) Kamieńska-Trela, K.; Knieriem, B. INDO Calculations of *J(CC)* and *J(CSi)* in Silyl Derivatives of acetylene and Diacetylene. *J. Organomet. Chem.* **1980**, *198*, 25–28.

(72) Hölzl, F.; Wrackmeyer, B. NMR-untersuchungen an einigen 1,3-diinen. *J. Organomet. Chem.* **1979**, *179*, 397–401.

(73) Kamieńska-Trela, K.; Ilcewicz, H.; Barańska, H.; Łabudzińska, A. The Raman, IR and ^{13}C-NMR Spectra of Triethylgermylacetylene, Bis(triethylgermyl)diacetylene and Their ^{13}C Labelled Analogues. *Bull. Pol. Acad. Sci. Chem.* **1984**, *32*, 143–150.

(74) Kamieńska-Trela, K.; Gluziński, P. Total Range of CC Coupling Constants in Diacetylene Derivatives Calculated by INDO FTP Method. *Croat. Chim. Acta.* **1986**, *59*, 883–890.

(75) Kamieńska-Trela, K.; Kania, L.; Schilf, W.; Balova, I. One-bond 13C−13C couplings in diacetylenes: experimental and theoretical studies. *Spectrochim. Acta, Part A* **1999**, *55*, 817–824.

(76) Taft, R. W.; Price, E.; Fox, I. R.; Lewis, I. C.; Andersen, K.; Davis, G. T. Fluorine Nuclear Magnetic Resonance Shielding in p-Substituted Fluorobenzenes. The Influence of Structure and Solvent on Resonance Effects. *J. Am. Chem. Soc.* **1963**, *85*, 3146–3156.

(77) Robinson, C. N.; Slater, C. D.; Covington, J. S., III; Chang, C. R.; Dewey, L. S.; Franceschini, J. M.; Fritzsche, J. L.; Hamilton, J. E.; Irving, C. C., Jr.; Morris, J. M.; Norris, D. W.; Rodman, L. E.; Smith, V. I.; Stablein, G. E.; Ward, F. C. Carbon-13 NMR chemical shift—Substituent effect correlations in substituted styrenes. *J. Magn. Reson.* **1969**, *41*, 293–301.

(78) Biedrzycka, Z.; Kamieńska-Trela, K.; Witanowski, M. Origin of significant solvent effects on ^{1}J(CC) spin−spin coupling in some acetylenes: hydrogen bonding and solvent polarity. *J. Phys. Org. Chem.* **2010**, *23*, 483–487.

(79) Kamieńska-Trela, K. One-bond ^{13}C−^{13}C spin coupling constants. *Annu. Rep. NMR Spectrosc.* **1995**, *30*, 131–230.

(80) Kamieńska-Trela, K.; Dąbrowski, A.; Januszewski, H. One-bond CC spin-spin coupling constants in derivatives of benzene. Nonlinearity of ^{1}J(CC) vs substituent electronegativity. *Spectrochim. Acta, Part A* **1993**, *49A*, 1613–1619.

(81) Biedrzycka, Z.; Kamieńska-Trela, K. The linear relationship between the one bond spin-spin coupling constants $^{1}J_{C\equiv C}$ and the product of the electronegativities Ex•Ey of substituents at the CC triple bond. *Spectrochim. Acta, Part A* **1986**, *42A*, 1323–1327.

(82) Biedrzycka, Z.; Kamieńska-Trela Influence of Substituents on Carbon-Carbon Coupling Constants in Substituted Acetylenes. *Pol. J. Chem.* **2003**, *77*, 1637–1648.

(83) Cremer, D.; Elfi Kraka, E.; Wu, A.; Lüttke, W. Can One Assess the π Character of a C - C Bond with the Help of the NMR Spin - Spin Coupling Constants? *Chem. Phys. Chem.* **2004**, *5*, 349–366.